

This work was written as part of one of the author's official duties as an Employee of the United States Government and is therefore a work of the United States Government. In accordance with 17 U.S.C. 105, no copyright protection is available for such works under U.S. Law.

Public Domain Mark 1.0

<https://creativecommons.org/publicdomain/mark/1.0/>

Access to this work was provided by the University of Maryland, Baltimore County (UMBC) ScholarWorks@UMBC digital repository on the Maryland Shared Open Access (MD-SOAR) platform.

Please provide feedback

Please support the ScholarWorks@UMBC repository by emailing scholarworks-group@umbc.edu and telling us what having access to this work means to you and why it's important to you. Thank you.



This discussion paper is/has been under review for the journal Atmospheric Measurement Techniques (AMT). Please refer to the corresponding final paper in AMT if available.

Direct sun and airborne MAX-DOAS measurements of the collision induced oxygen complex, O₂O₂ absorption with significant pressure and temperature differences

**E. Spinei^{1,2,5}, A. Cede^{3,2}, J. Herman^{4,2}, G. H. Mount⁵, E. Eloranta⁶, B. Morley⁷,
S. Baidar^{8,9}, B. Dix⁸, I. Ortega^{8,9}, T. Koenig^{8,9}, and R. Volkamer^{8,9}**

¹ESSIC, University of Maryland, College Park, MD, USA

²NASA/Goddard Space Flight Center (GSFC), Greenbelt, MD, USA

³Universities Space Research Association, Greenbelt, MD, USA

⁴University of Maryland, Baltimore County (UMBC), Catonsville, MD, USA

⁵Laboratory for Atmospheric Research, Washington State University (WSU), Pullman WA, USA

⁶Space Science and Engineering Center, University of Wisconsin, Madison, WI, USA

⁷Earth Observing Laboratory, National Center for Atmospheric Research, Boulder, CO, USA

⁸Dept. of Chemistry and Biochemistry, University of Colorado, Boulder, CO, USA

Absorption with significant pressure and temperature differences

E. Spinei et al.

Title Page

Abstract

Introduction

Conclusions

References

Tables

Figures

[Back](#)

Close

Full Screen / Esc

[Printer-friendly Version](#)

Interactive Discussion



⁹CIRES, University of Colorado, Boulder, CO, USA

Received: 17 July 2014 – Accepted: 4 September 2014 – Published: 26 September 2014

Correspondence to: E. Spinei (espinei@wsu.edu)

Published by Copernicus Publications on behalf of the European Geosciences Union.

AMTD

7, 10015–10057, 2014

Absorption with significant pressure and temperature differences

E. Spinei et al.

Title Page

Abstract

Introduction

Conclusions

References

Tables

Figures

◀

▶

◀

▶

Back

Close

Full Screen / Esc

Printer-friendly Version

Interactive Discussion



Abstract

The collision induced O_2 complex, O_2O_2 , is a very important trace gas in remote sensing measurements of aerosol and cloud properties. Some ground based MAX-DOAS measurements of O_2O_2 slant column density require correction factors of 0.75 ± 0.1 to reproduce radiative transfer modeling (RTM) results for a near pure Rayleigh atmosphere. One of the potential causes of this discrepancy is believed to be uncertainty in laboratory measured O_2O_2 absorption cross section temperature and pressure dependence, due to difficulties in replicating atmospheric conditions in the laboratory environment.

This paper presents direct-sun (DS) and airborne multi-axis (AMAX) DOAS measurements of O_2O_2 absorption optical depths under actual Earth atmospheric conditions in two wavelength regions (335–390 nm and 435–490 nm). DS irradiance measurements were made by the research grade MFDOAS instrument from 2007–2014 at seven sites with significant pressure (778–1013 hPa) and O_2O_2 profile weighted temperature (247–275 K) differences. Aircraft MAX-DOAS measurements were conducted by the University of Colorado AMAX-DOAS instrument on 29 January 2012 over the Southern Hemisphere subtropical Pacific Ocean. Scattered solar radiance spectra were collected at altitudes between 9 and 13.2 km, with O_2O_2 profile weighted temperatures of 231–244 K, and near pure Rayleigh scattering conditions.

Due to the well defined DS air mass factors and extensively characterized atmospheric conditions during the AMAX-DOAS measurements, O_2O_2 “pseudo” absorption cross sections, σ , are derived from the observed optical depths and estimated O_2O_2 column densities. Vertical O_2O_2 columns are calculated from the atmospheric sounding temperature, pressure and specific humidity profiles.

Based on the atmospheric DS observations, there is no pressure dependence of the O_2O_2 σ , within the measurement errors (3 %). The two data sets are combined to derive peak σ temperature dependence of 360 and 477 nm absorption bands from 231–275 K. DS and AMAX derived peak $\sigma(O_2O_2)$ as a function of T can be described

AMTD

7, 10015–10057, 2014

Absorption with significant pressure and temperature differences

E. Spinei et al.

Title Page

Abstract

Introduction

Conclusions

References

Tables

Figures

◀

▶

◀

▶

Back

Close

Full Screen / Esc

Printer-friendly Version

Interactive Discussion



by a quadratic function at 360 nm and linear at 477 nm with about $9 \pm 2.5\%$ per 44 K rate.

Recent laboratory measured O_2O_2 cross sections by Thalman and Volkamer (2013) agree with these “DOAS apparent” peak $\sigma(O_2O_2)$ at 233 K, 253 K and 273 K within 3 %.

Changes in the O_2O_2 spectral band-shape at colder temperatures are for the first time also observed in field data. Temperature effects on spectral band shapes can introduce errors in the retrieved O_2O_2 column abundances if a single room temperature $\sigma(O_2O_2)$ is used in the DOAS analysis. Simultaneous fitting of $\sigma(O_2O_2)$ at temperatures that bracket the ambient temperature range can reduce such errors.

Our results suggest that laboratory measured $\sigma(O_2O_2)$ (Hermans et al. (2011) at 296 K and Thalman and Volkamer (2013)) are applicable for observations over a wide range of atmospheric conditions. Column densities derived using Hermans et al. (2011) σ at 296 K require very small correction factors (0.94 ± 0.02 at 231 K and 0.99 ± 0.02 at 275 K) to reproduce theoretically calculated SCDs for DS and AMAX-DOAS measurements. Simultaneous fitting of $\sigma(O_2O_2)$ at 203 and 293 K further improved results at UV and visible wavelengths for AMAX-DOAS.

1 Introduction

O_2O_2 has been widely used in remote sensing to retrieve aerosol and cloud information from spectroscopic measurements using ground based (Wagner et al., 2002, 2004; Frieß et al., 2006; Irie et al., 2008, 2009; Clémer et al., 2010) and space instruments (Acarreta et al., 2004; Sneep et al., 2008). The advantage of O_2O_2 for such measurements is that its concentration is directly proportional to the square of the oxygen concentration (R1).



The nature of molecular interactions in the O_2O_2 collisional complex is still debated (Sneep et al., 2006) and the equilibrium constant, K_{eq} , in (R1) is not known. As a result,

Absorption with significant pressure and temperature differences

E. Spinei et al.

Title Page

Abstract

Introduction

Conclusions

References

Tables

Figures



Back

Close

Full Screen / Esc

Printer-friendly Version

Interactive Discussion



only the “pseudo”, not the true concentration of the O_2O_2 collisional complex can be determined. After application of the ideal gas law the “pseudo” O_2O_2 column are easily calculated when atmospheric temperature, pressure and specific humidity profiles are known.

5 O_2O_2 absorption) can be accurately measured by the differential optical absorption spectroscopy (DOAS) technique due to several absorption bands in the UV and visible parts of the spectrum (e.g., $\approx 343, 360, 380, 477, 532, 577, 630$ nm, Wagner et al., 2002) assuming availability of accurate “pseudo” absorption cross section, σ , as a function of T and P . The problem with the laboratory measurements of σ is related to the
10 need to have long paths and/or higher pressures compared to atmospheric conditions for sufficient absorption. Despite numerous laboratory measurements of $\sigma(\text{O}_2\text{O}_2)$ in UV and visible spectral regions (Salow and Steiner, 1934; Greenblatt et al., 1990; Volkamer, 1996; Newnham and Ballard, 1998; Hermans et al., 2011; Snee and Ubachs, 2003; Snee et al., 2006; Thalman and Volkamer, 2013), the question of their applicability to atmospheric conditions remains unanswered. Only Thalman and Volkamer
15 (2013) made $\sigma(\text{O}_2\text{O}_2)$ laboratory measurements at the pressure close to ambient (825 hPa). Their $\sigma(\text{O}_2\text{O}_2)$ at 295 K agree with the Hermans et al. (2011) $\sigma(\text{O}_2\text{O}_2)$ at 296 K within the instrumental measurement errors. The main confusion arises from the fact that under low aerosol conditions approaching a near pure Rayleigh atmosphere
20 multi axis DOAS measurements (MAX-DOAS) of O_2O_2 differential slant column density, ΔSCD , require a “correction factor” of about 0.75–0.89 to reproduce the O_2O_2 ΔSCD modeled by different radiative transfer algorithms while using Hermans et al. (2011) $\sigma(\text{O}_2\text{O}_2)$ at 296 K (Table 1).

Absorption with significant pressure and temperature differences

The σ dependence on temperature potentially originates from two sources: temperature dependence of K_{eq} and temperature dependence of the true absorption cross section. Pfeilsticker et al. (2001) assumed that temperature dependence is solely due to K_{eq} . Thalman and Volkamer (2013) demonstrated that the integral of the stronger absorption lines is temperature independent, while the line shape and peak values exhibit some temperature dependence.



**Absorption with
significant pressure
and temperature
differences**

E. Spinei et al.

Title Page

Abstract

Introduction

Conclusions

References

Tables

Figures

◀

▶

◀

▶

Back

Close

Full Screen / Esc

Printer-friendly Version

Interactive Discussion



In this study we investigate the pressure and temperature dependence of the cross section peak values and line shape using actual field DOAS measurements of O_2O_2 optical depth. We further assess the bias introduced by the temperature dependence of σ (O_2O_2) on the DOAS fit, and discuss a possible solution. Using non-scattered direct-sun (DS) photons for σ measurements is very desirable, since O_2O_2 optical depth is observed under actual atmospheric conditions and the photon path is well defined. Aircraft measurements in the free troposphere are advantageous, since they detect mainly Rayleigh scattered photons and facilitate a more straightforward comparison with Radiative Transfer Model (RTM) calculations.

This study presents O_2O_2 “DOAS apparent” cross sections derived from DS and airborne MAX-DOAS (AMAX-DOAS) measurements for the 335–390 and 435–490 nm wavelength ranges. Pressure dependence was evaluated from DS data collected at three sites with roughly the same O_2O_2 effective temperature (~ 266 K) and pressures of 780, 925 and 1013 hPa. Temperature dependence of O_2O_2 σ was examined from the ground-based DS and AMAX-DOAS measurements. DS data were collected at seven sites where O_2O_2 T ranged from 247–275 K. AMAX-DOAS measurements were made between 9 and 13.2 km at near pure Rayleigh scattering conditions with O_2O_2 T between 232 and 244 K.

The paper is organized in the following sections. Section 2 explains the methodology to calculate the normalized VOD and peak O_2O_2 cross section using the DOAS technique. Section 3 describes the DS and AMAX-DOAS instrumentation, measurement sites and DOAS settings. Section 4 presents results. Conclusions are outlined in Sect. 5.

2 Methodology

2.1 DOAS

Differential optical absorption spectroscopy (DOAS) for weak absorbers is based on the modified Beer–Lambert law which describes solar radiation attenuation due to molecular and aerosol absorption and scattering, Eq. (1) (Platt, 1994; Danckaert et al., 2012). DOAS separates the strongly wavelength dependent molecular absorption cross-section structure ($\sigma'_i(\lambda)$) of the absorbing gases from the weak wavelength dependence of the aerosol and molecular scattering and absorption (wide band extinction).

$$\ln(I_{\text{ref}}(\lambda)) - \ln(I(\lambda) - \text{offset}(\lambda)) = \underbrace{\left[\sum_s (\sigma'_i(\lambda) \cdot \Delta\text{SCD}_i) \right]}_{\text{dif. absorption}} + P_{\text{Lo}} \quad (1)$$

The DOAS technique does not require prior knowledge of Rayleigh and aerosol extinction to derive differential slant column densities (ΔSCD_i) of a gas i , since the wide band extinction can be approximated by a low-order polynomial function (P_{Lo}). Unwanted instrumental stray light is removed as an offset term in Eq. (1). ΔSCD_i , the low-order polynomial function and offset are simultaneously fitted by a non-linear least squares algorithm to the difference between the logarithms of the attenuated (I) and reference (I_{ref}) spectra. The reference spectrum used in DOAS analysis is typically a solar spectrum measured by the same instrument under the lowest available slant path and abundance conditions.

The total vertical column density (CD) measured in any DOAS observation geometry is related to ΔSCD according to Eq. (2), where SCD_{REF} is the SCD in the reference spectrum and the air mass factor (AMF) is the photon path enhancement relative to the

Absorption with significant pressure and temperature differences

E. Spinei et al.

Title Page

Abstract

Introduction

Conclusions

References

Tables

Figures

◀

▶

◀

▶

Back

Close

Full Screen / Esc

Printer-friendly Version

Interactive Discussion



vertical direction.

$$CD = \frac{\Delta SCD + SCD_{REF}}{AMF} \quad (2)$$

The AMF for DS measurements is almost wavelength independent for most solar zenith angles (SZA) and can be easily estimated using the geometrical approximation, that is roughly equal to $1/\cos(SZA)$ (for the equation used in this study see Cede et al., 2006). For weak absorbers with an almost constant vertical CD, such as O_2O_2 , an increase in ΔSCD from DS measurements is mainly due to an increase in the photon path length (AMF). For this type of absorbers, the Langley Plot method is used to estimate SCD_{REF} .

For MAX-DOAS measurements the AMF is wavelength dependent and is a function of atmospheric composition and scattering conditions and requires RTM. The main complication in MAX-DOAS AMF calculations arises from insufficient knowledge of aerosol micro/macro properties and spatial distribution. This is not a problem for modeling of a pure Rayleigh atmosphere.

To simplify further discussion we introduce a specific notation that is followed through the remainder of the paper.

1. All quantities that exhibit strong wavelength dependence are depicted as vectors:

σ – O_2O_2 “pseudo” absorption cross section [cm^5 molecule $^{-2}$];

τ – O_2O_2 “pseudo” absorption optical depth, $\tau = \sigma \cdot CD$;

2. All quantities that exhibit very small or no wavelength dependence are expressed as scalars:

CD – “pseudo” column density derived from a specific fitting window [molecule 2 cm $^{-5}$];

3. All “true” or theoretically estimated quantities from the “true” measurements are expressed using “*” superscript:

Absorption with significant pressure and temperature differences

E. Spinei et al.

Title Page

Abstract

Introduction

Conclusions

References

Tables

Figures

◀

▶

◀

▶

Back

Close

Full Screen / Esc

Printer-friendly Version

Interactive Discussion



CD* – “pseudo” column density calculated from the temperature (T), pressure (P) and specific humidity (SH) profiles [$\text{molecule}^2 \text{cm}^{-5}$];

τ^* – theoretical O_2O_2 “pseudo” absorption optical depth: $\tau^* = \sigma \cdot \text{CD}^*$;

T^* – O_2O_2 “pseudo” profile and box-AMF weighted effective temperature [K];

4. Differential quantities are expressed using a “ Δ ” prefix;
5. Quantities integrated along the photon path (slant) are expressed using an “S” prefix, quantities integrated along the vertical direction (vertical) have no prefix notation;

6. Quantities describing the reference spectrum are expressed using “REF” as subscript:

CD_{REF} – CD in the reference spectrum;

T_{REF}^* – O_2O_2 “pseudo” profile weighted effective temperature at the reference time [K];

τ_{REF} – O_2O_2 “pseudo” absorption optical depth in the reference spectrum;

7. The word “pseudo” is omitted while referring to O_2O_2 parameters.
8. Goodness of the linear fit between two quantities is expressed as the coefficient of determination (R^2). R^2 is rounded to two or three decimal places. In case of $R^2 = 1.00$ or 1.000 less than 0.5 % or 0.05 % of the variation cannot be explained by the linear model.

2.2 Pressure and temperature dependence

The DOAS technique can be applied to evaluate pressure and temperature dependence of a laboratory measured molecular absorption cross section for gases with known CD^* , using remote sensing atmospheric observations with well defined AMFs.

Absorption with significant pressure and temperature differences

E. Spinei et al.

Title Page

Abstract

Introduction

Conclusions

References

Tables

Figures

◀

▶

◀

▶

Back

Close

Full Screen / Esc

Printer-friendly Version

Interactive Discussion



This is accomplished by evaluating the normalized τ (Eq. 3) calculated from the DOAS fitted radiance/irradiance as a function of T or P (Wagner et al., 2002).

$$\sigma(T^*, P) = \frac{\tau}{CD^*} = \left(\frac{\Delta s\tau + s\tau_{\text{REF}} + \tau_{\text{RESIDUAL}}}{AMF} \right) \cdot \frac{1}{CD^*} \quad (3)$$

5 Where:

- $\Delta s\tau$ is the DOAS fitted O_2O_2 τ at effective measurement temperature T^* and pressure P , and is equal to the product of O_2O_2 ΔSCD and laboratory measured σ used in the DOAS analysis: $\Delta s\tau = \Delta\text{SCD} \cdot \sigma$;
- $s\tau_{\text{REF}}$ is O_2O_2 slant τ in the reference spectrum ($s\tau_{\text{REF}} = \text{SCD}_{\text{REF}} \cdot \sigma$) at T_{REF}^* and pressure P_{REF} , with the SCD_{REF} derived using the Langley Plot method from a single “reference” day;
- τ_{RESIDUAL} is the residual optical depth that is not attributed to any known absorption by the DOAS analysis at wavelength λ in each measurement.

15 The main assumption of the approach is that OD of all species absorbing in the specific wavelength window are accounted for and the residual OD is only due to the variation in the cross section of the species of interest.

Any significant differences in shape between the true O_2O_2 cross section and the fitted σ should be captured in the residual optical depth. “Broad” differences will be “masked” by the combination of the polynomial and offset fits. As a result the derived cross section in Eq. (3) is a “DOAS apparent” cross section which might not exactly match the true cross section.

20 In this study, the QDOAS software package (Danckaert et al., 2012) is used to derive the ΔSCD and τ from DS measurements and WinDOAS (Fayt and Van Roozendaal, 2001) for the analysis of aircraft measurements.

25 To evaluate a potential pressure dependence of σ , we use a DS Fraunhofer spectrum, measured at a higher altitude (lower pressure) location, as a reference spectrum

Absorption with significant pressure and temperature differences

E. Spinei et al.

Title Page

Abstract

Introduction

Conclusions

References

Tables

Figures

◀

▶

◀

▶

Back

Close

Full Screen / Esc

Printer-friendly Version

Interactive Discussion



to analyze DS data collected at lower altitudes (higher pressure). The main requirements are high signal to noise ratio in the measurements at all locations and the same $O_2O_2 T^*$. DOAS derived $\Delta SCDs$ are then compared to ΔSCD^* estimated from T , P and SH profiles at the corresponding sites.

To evaluate temperature dependence of σ , both DS and AMAX-DOAS data are used. For DS observations a reference Fraunhofer spectrum measured at the smallest SZA is applied to the data collected at the same site. For the AMAX-DOAS measurements, a spectrum, collected at ceiling altitude (13.2 km) pointing 10° above horizontal direction ($EA 10^\circ$), is used as a reference Fraunhofer spectrum.

3 Data description, DOAS and radiative transfer settings

3.1 Direct sun measurements

DS spectra were measured by the Multi-Function Differential Spectroscopy Instrument (MFDOAS) (Herman et al., 2009) in the wavelength region 282–498 nm at seven sites: Table Mountain – JPL facility, CA (JPL); University of Alabama, Huntsville (UAH); Cabauw, the Netherlands; University of Alaska in Fairbanks (UAF); Washington State University (WSU), Pullman, WA (WSU); Pacific Northwest National Laboratory (PNNL), Richland, WA and Goddard Space Flight Center (GSFC/NASA), Greenbelt, MD. Temperature, pressure and specific humidity profiles were composed for each site from the following sources to ensure consistent vertical CD^* calculation from the surface to the TOA:

- surface pressure, temperature and relative humidity measured by Vaisala Weather Transmitter WXT520;
- radio soundings launched at nearby sites twice a day (00:00 and 12:00 UTC, available at <http://weather.uwyo.edu/upperair/sounding.html>). During some field campaigns frequent ozonesonde measurements were also available (UAF, JPL, UAH).

- Modern Era Retrospective-Analysis for Research and Applications (MERRA, <http://gmao.gsfc.nasa.gov/merra/>) T , P and SH profiles (instantaneous 6 h).

Table 2 summarizes average O_2O_2 CD* and T^* calculated for each site from the T , P and SH profiles.

The MFDOAS instrument combines measurements of DS irradiance and scattered sun radiance (MAX-DOAS). DS photons are collected by a telescope with a 1.4° field of view (FOV) and are guided through the 8 cm diameter spectralon integrating sphere. The integrating sphere assures uniform illumination of the spectrometer optics and minimizes the effect of FOV pointing inaccuracy. A modified 300 mm-focal length single pass Czerny–Turner spectrometer from Acton Research, Inc. (SpectraPro-2356) is used to disperse light. A 400 groove per mm ruling grating blazed at 400 nm is installed in the grating turret. Light enters the spectrometer through a $100\ \mu\text{m}$ slit. The baffling internal to this spectrograph has been substantially modified to eliminate reentrant light and scattering artifacts. A charge-coupled device (CCD) from Princeton Instruments (PIXIS: 2KBV) is used to detect the spectrally dispersed light. It has an enhanced UV sensitivity due to back-illumination and UV coating. The imaging area is composed of 512 rows by 2048 columns of square pixels ($13.5 \times 13.5\ \mu\text{m}^2$). MFDOAS has an average spectral resolution of 0.83 nm with a sampling of 7.83 pixels per full width at half maximum.

MFDOAS spectra were analyzed in two wavelength regions 335–390 nm and 435–490 nm to evaluate the ~ 360 and 477 nm absorption lines. Table 3 lists all fitting parameters and laboratory measured higher resolution molecular absorption cross sections used in DOAS analyses after convolution with the MFDOAS instrument transfer function. All cross sections were fitted as non-differential cross sections to remove dependence on the polynomial order used to estimate cross section broad band absorption. To evaluate DOAS errors associated with the fitting parameters we varied the wavelength fitting windows (435–485, 435–490, 450–485, 350–385, 335–370, 335–390 nm), polynomial order (3, 4 and 5) and offset order (0 and 1).

Absorption with significant pressure and temperature differences

E. Spinei et al.

Title Page

Abstract

Introduction

Conclusions

References

Tables

Figures

◀

▶

◀

▶

Back

Close

Full Screen / Esc

Printer-friendly Version

Interactive Discussion



Absorption with significant pressure and temperature differences

E. Spinei et al.

Title Page

Abstract

Introduction

Conclusions

References

Tables

Figures

◀

▶

◀

▶

Back

Close

Full Screen / Esc

Printer-friendly Version

Interactive Discussion



A single, site specific, reference Fraunhofer spectrum was selected to analyze all the data available at the corresponding site (for the same instrument configuration). This reference spectrum was calculated as an average of spectra collected during a 30 min interval around a small SZA. Since O_2O_2 CD^* can vary by a few percent during a particular day due to diurnal pressure/temperature changes only days with relatively constant surface P were selected as reference days. Langley plot method to derive SCD_{REF} was applied only to the DS spectra collected during these reference days.

Pressure dependence was examined by using a reference spectrum measured at JPL located at 2.3 km a.s.l. with surface pressure of 780 hPa to analyze data collected at WSU (925 hPa) and GSFC (1013) with O_2O_2 $T^* \approx 266$ K.

3.2 AMAX-DOAS measurements of O_2O_2 in a near pure Rayleigh atmosphere

The TORERO field experiment (Tropical Ocean tRoposphere Exchange of Reactive halogen species and Oxygenated VOC, January–February 2012) provided an opportunity to measure and assess O_2O_2 absorption in a Rayleigh atmosphere by means of the University of Colorado airborne MAX-DOAS instrument (Baidar et al., 2013). TORERO deployed a unique selection of chemical in-situ and remote sensing instruments aboard the National Science Foundation/National Center for Atmospheric Research Gulfstream V aircraft (NSF/NCAR GV) over the Eastern Pacific Ocean. We have measured ambient temperature, pressure, water vapor and ozone (all by in-situ sensors), aerosol size distributions by an Ultra High Sensitivity Aerosol Spectrometer (UHSAS), as well as temperature profiles by the Microwave Temperature Profiler (MTP) (Denning et al., 1989; Lim et al., 2012), and aerosol extinction profiles by High Spectral Resolution LIDAR (HSRL, Eloranta et al., 2008). Four cameras provide information on cloudiness forward, sideways, and below the aircraft. Research flight 05 (RF05) was conducted on 29 January 2012 from/to Antofagasta, Chile over the Southern Hemisphere subtropical Pacific Ocean, where the aircraft probed very clear air during a case study from 18:06–18:30 UTC (9–13.2 km altitude; SZA of 12.4–12.0°, 92.4–92.1° E/29.7–29.9° S).

Absorption with significant pressure and temperature differences

E. Spinei et al.

Title Page

Abstract

Introduction

Conclusions

References

Tables

Figures

◀

▶

◀

▶

Back

Close

Full Screen / Esc

Printer-friendly Version

Interactive Discussion



The ambient temperature varied from 235.4–214.3 K. The corresponding O₂O₂ effective temperatures, calculated for 360/477 nm using box-AMFs and measured T , P , SH, ranged from 243.4/239.3–235.3 K/232.4 K (see Table 2). The camera data shows only sparsely scattered boundary layer clouds. The aerosol extinction profile measured by the HSRL at 532 nm showed sub-Rayleigh aerosol extinction values above the aircraft. The aerosol content in the stratosphere was nominally zero, i.e. the measured aerosol backscatter cross section is too small to derive any extinction values. Below the aircraft, aerosol extinction was sub-Rayleigh above 1.5 km, and agreed very well (better 0.01 km⁻¹) with Mie calculations below 1.5 km (see Fig. 1). Mie calculations were constrained by measured size distributions, and used to better quantify the low aerosol extinction values in the free troposphere, FT, as well as to estimate the wavelength dependence of aerosol extinction at the O₂O₂ wavelengths. The mean aerosol number density between 9 and 13.2 km was $5.8 \pm 1.7 \text{ cm}^{-3}$. The average aerosol size distribution over this altitude range had an effective radius, $R_e = 0.11 \pm 0.02 \mu\text{m}$. Mie code was initiated assuming a constant refractive index, n , at all sizes and wavelength dependencies as described in Massie and Hervig (2013). Sensitivity studies varied $n \sim 1.55$ (sea salt), ~ 1.30 (ice) and ~ 1.56 (mineral dust). The aerosol extinction values (sea salt) averaged between 9 and 13.2 km are $4.6 \times 10^{-4} \text{ km}^{-1}$ (532 nm), $5.2 \times 10^{-4} \text{ km}^{-1}$ (477 nm), and $6.7 \times 10^{-4} \text{ km}^{-1}$ (360 nm), respectively. These numbers are 1 to 2 orders of magnitude lower than the extinction due to molecular (Rayleigh) scattering at the O₂O₂ wavelengths (see Fig. 1). The atmospheric radiation state can be described in good approximation as a Rayleigh atmosphere.

AMAX-DOAS measures scattered sunlight spectra from well-defined lines of sight. The limb scanning telescope has a FOV of 0.17° and is actively angle stabilized to better 0.2° accuracy in real time (Baidar et al., 2013; Dix et al., 2013). Two synchronized spectrograph-detector units (Acton SP2150/PIXIS400B CCD) simultaneously observed the spectral ranges from 330–470 nm (0.7 nm Full Width Half Maximum (FWHM) optical resolution) and 430–680 nm (1.2 nm FWHM optical resolution). O₂O₂ ΔSCDs were retrieved by application of a non-linear least squares DOAS fitting routine

Absorption with significant pressure and temperature differences

E. Spinei et al.

Title Page

Abstract

Introduction

Conclusions

References

Tables

Figures

◀

▶

◀

▶

Back

Close

Full Screen / Esc

Printer-friendly Version

Interactive Discussion



using the WinDOAS software package (Fayt and van Roozendaal, 2001) for two wave-length windows: 350–387.5 nm (with a gap between 366 and 374.5 nm to minimize Ring effect) and 445–485 nm using (1) the Hermans cross section at 296 K (Hermans et al., 2011) and (2) the Thalman and Volkamer cross sections at 293 K and 203 K (Thalman and Volkamer, 2013). These analysis settings are optimized to retrieve robust Δ SCDs over the wide range of atmospheric conditions encountered during a typical 8 h flight time. A summary of analysis settings and cross sections used can be found in Table 3. One spectrum collected at 13.2 km altitude was used as a reference Fraunhofer spectrum to analyze all data (see Table 2). The reference elevation angle is upward looking (EA 10°) to minimize the slant column amount contained in the reference, SCD_{REF} . Spectra were measured with elevation angle (EA) 0° (i.e. horizontal and parallel to flight altitude) during ascent; further three upward angle scans (1°, 2°, 5°) at constant flight altitude (13.2 km) were included in the analysis.

Radiative transfer calculations were performed with McArtim (Deutschmann et al., 2011), a fully spherical Monte Carlo RTM, for 360 and 477 nm. Radiation fields were constrained by in-situ pressure, temperature, water vapor, ozone, MTP temperature profiles, and stratospheric profiles of NO₂ and O₃ taken from the Real-time Air Quality Modeling System (RAQMS) (Piers et al., 2007). The O₂O₂ vertical profile was calculated as the square of the O₂ concentration based on measured temperature and pressures and corrected for water vapor concentration. Ocean surface albedo was set to 5 % at 360 nm and to 8 % at 477 nm. Solar and observation geometry were input variables for the RTM.

4 Results and discussion

4.1 O₂O₂ reference slant optical depth in direct sun and AMAX-DOAS measurements

Estimation of $s\tau_{\text{REF}}$ in Eq. (3) requires determination of SCD_{REF} from DS and AMAX-DOAS data. SCD_{REF} are calculated from the DOAS fitted ΔSCD using Hermans et al. $\sigma(\text{O}_2\text{O}_2)$ at 296 K by applying the Langley Plot method. SCD_{REF} is then multiplied by σ to determine $s\tau_{\text{REF}}$.

4.1.1 Direct sun measurements

SCD_{REF} were calculated from the DS measurements at each site in the UV and visible fitting windows using the Langley plot method. Figure 2 shows Langley plots for the reference data analyzed in 435–490 nm with the settings described in Table 3. Linear regression analysis shows high correlation between the DS ΔSCD and ΔAMF with R^2 of 1.000 for the visible wavelength region and better than 0.980 for UV. The final error in the SCD_{REF} derived from the UV and visible wavelength windows was determined as one standard deviations of SCD_{REF} calculated from ΔSCDs with different DOAS fitting parameters (e.g. polynomial order, offset order, fitting window boundaries). The estimated relative error in SCD_{REF} from the visible wavelength region is about 1 % and from the UV wavelengths is about 2.4 %. Derived SCD_{REF} from DS measurements agree with the $\text{SCD}_{\text{REF}}^*$ within these errors.

4.1.2 AMAX-DOAS measurements

SCD_{REF} in the AMAX reference Fraunhofer spectrum, measured at 13.2 km and 10° EA, was calculated from the linear correlation between the measured ΔSCD and modeled SCD^* at 360 and 477 nm assuming pure Rayleigh scattering conditions (Fig. 3, upper panel). SCD^* accounted for an altitudinal dependence of O_2O_2 CD^* . The slant column amount contained in the reference, SCD_{REF} , is the absolute value of

Absorption with significant pressure and temperature differences

E. Spinei et al.

Title Page

Abstract

Introduction

Conclusions

References

Tables

Figures

◀

▶

◀

▶

Back

Close

Full Screen / Esc

Printer-friendly Version

Interactive Discussion



the intercept. Linear regression parameters are summarized in Table 4. The modeled SCD_{REF} values agree with the SCD_{REF} inferred from the measurements within 1.7 % at 360 nm and 1.6 % at 477 nm. The slope of the linear correlation is expected to be unity if there is no temperature dependence of $\sigma(O_2O_2)$, and atmospheric conditions are correctly described by the model. Given the small temperature dependence of the O_2O_2 cross section shape (Thalman and Volkamer, 2013) some deviation from “1” is expected while fitting $\sigma(O_2O_2)$ at a single T. The observed divergences from “1” are 2.9 % at 360 nm and 1.6 % at 477 nm

To evaluate the effect of aerosol extinction below the aircraft on the linear correlation between the measured ΔSCD and estimated SCD^* (SCD_{REF} and slope), we recalculated AMFs and SCD^* including the extinction profiles derived from Mie theory. In the RTM aerosols are described by single scattering albedo (0.97 at 360 nm, 0.98 at 477 nm) and g-parameter (0.75–0.7 for 0–13 km). The extinction profile is taken from the Mie calculations for the sea salt case (see Fig. 1). For the aerosol scenario, agreement between the measured SCD_{REF} and estimated SCD_{REF}^* slightly improves (0.9 % at 360 nm and 0.8 % at 477 nm), but slope deviations from “1” increase to 5.2 ± 5 % at 360 nm and 2.6 ± 1 % at 477 nm.

4.2 $\sigma(O_2O_2)$ pressure dependence from DS measurements

To investigate the effect of pressure on the O_2O_2 VOD we used the Fraunhofer reference spectrum collected over JPL (7 July 2007) to analyze the reference spectra collected over WSU, Pullman, WA (11 September 2007) and GSFC, Greenbelt, MD (23 May 2007). The estimated ΔSCD^* over WSU relative to JPL reference column is 0.667×10^{43} molecules² cm⁻⁵, and over GSFC is 0.579×10^{43} molecules² cm⁻⁵. These estimations are determined based on the calculated CD^* from T, P, SH profiles and AMFs of the corresponding measurements.

DOAS retrieved ΔSCD from 435–490 nm window in the WSU spectrum from 11 September 2007 and in GSFC spectrum from 23 May 2007 relative to JPL reference spectrum from 7 July 2007 were (0.665 ± 0.007) and $(0.574 \pm$

$0.008) \times 10^{43} \text{ molecules}^2 \text{ cm}^{-5}$ respectively. Residual OD RMS were small (1.39 and 1.55×10^{-4}) without any significant spectral structure. Corresponding ΔSCD retrieved in the $335\text{--}392 \text{ nm}$ fitting region were (0.688 ± 0.014) and $(0.579 \pm 0.014) \times 10^3 \text{ molecules}^2 \text{ cm}^{-5}$. Residual ODs in UV were about two times larger than in visible due to smaller signal-to-noise ratio (SNR) in the UV part of the MFDOAS spectrum compared to the visible. Some of the residual structure in UV is probably the result of incomplete removal of stray light due to scattering of photons with longer wavelength within the spectrograph. Hoya U340 filter was added after 2008 to improve SNR in the UV.

Figure 4 shows DOAS apparent $\sigma(\text{O}_2\text{O}_2)$ estimated from the T , P , SH profiles at the two sites. The agreement between the derived $\sigma(\text{O}_2\text{O}_2)$ at 1013 and 925 hPa (relative to 780 hPa) and Hermans laboratory measured $\sigma(\text{O}_2\text{O}_2)$ at 296 K (after convolution with MFDOAS ITF) is better than 3%. We conclude that $\sigma(\text{O}_2\text{O}_2)$ does not exhibit a pressure sensitivity between 780 and 1013 hPa within typical DOAS instrumental and fitting errors.

4.3 Temperature dependence of observed $\tau(\text{O}_2\text{O}_2)$

Since no pressure dependence was observed between 780 and 1013 hPa, we combined data from all sites for DS and from AMAX-DOAS measurements to determine the temperature dependence of $\sigma(\text{O}_2\text{O}_2)$. O_2O_2 from DS measurements (Eq. 3) were averaged to produce single daily values. CD^* calculated from T , P and SH profiles were interpolated on a DS daily time grid. The AMAX-DOAS data were binned and averaged within 2 K increments to derive vertical column densities. CD^* was calculated from simultaneous in-situ temperature and pressure measurements, corrected by in-situ water vapor data. Above the aircraft the temperature profile was extended using MTP data and RAQMS model pressure.

Figure 5 provides an example of the of the AMAX-DOAS spectral fit in the UV and visible windows for O_2O_2 effective temperatures of $239.7 \pm 0.4 \text{ K}$ at 360 and $234.8 \pm 0.5 \text{ K}$

477 nm agrees with the results presented here within the measurement errors. Wagner et al. (2002) O_2O_2 peak σ (242 K) are 25 % and 12 % larger than the derived values in this study for 360 and 477 nm correspondently.

4.4 Accounting for temperature dependence of measured $\tau(\text{O}_2\text{O}_2)$ in DOAS fit

5 Given the relatively cold O_2O_2 effective temperatures of the AMAX-DOAS measurements ($\sim 231\text{--}244$ K) results are expected to improve by simultaneous DOAS fitting of two $\sigma(\text{O}_2\text{O}_2)$ cross sections (Thalman and Volkamer, 2013) at 293 K and 203 K. Figure 5 shows substantial reduction in the residual OD structures as well as decrease in the fitted ΔSCD (203 and 293 K combined) using this approach. This presents independent evidence from field observations that the spectral band shapes depend on temperature. Figure 3 and Table 4 also show effect of more accurately accounting for temperature dependence of σ on correlation between AMAX measured ΔSCD and modeled SCD. The results for Rayleigh and aerosol cases at 477 nm are comparable to fitting $\text{O}_2\text{O}_2\sigma$ at a single T within corresponding errors. The slopes are indistinguishable from unity and the SCD_{REF} are within less than 1 % of the modeled $\text{SCD}_{\text{REF}}^*$. Fitting two O_2O_2 cross sections has a more pronounced effect on the slope and SCD_{REF} at 360 nm. Derived slopes decrease both for pure Rayleigh and aerosol cases by about 7 %, which brings the slope for the aerosol case within 2 % of unity. While the temperature dependence in the combined ΔSCD vs. SCD^* is reduced the recalculated SCD_{REF} are slightly underestimated: by less than 7 % for pure Rayleigh case and 5 % for aerosol case.

Figure 8 shows measured VCD normalized by VCD^* in case of fitting one σ (Hermans et al., 2011, at 296 K) and two σ (Thalman and Volkamer, 2013, at 203 and 293 K) for DS and AMAX-DOAS measurements at 360 (A) and 477 nm (B). The inverse of the normalized VCD can be interpreted as “correction factors” necessary to bring the measured VCDs to “true” VCD^* . In case of fitting a single σ at 296 K the CFs are temperature-dependent and range from 1 ± 0.02 at 275 K to 0.94 ± 0.02 at 231 K for both UV and visible spectral regions. The effect of temperature to bias the

Absorption with significant pressure and temperature differences

E. Spinei et al.

Title Page

Abstract

Introduction

Conclusions

References

Tables

Figures

◀

▶

◀

▶

Back

Close

Full Screen / Esc

Printer-friendly Version

Interactive Discussion



Absorption with significant pressure and temperature differences

E. Spinei et al.

Title Page

Abstract

Introduction

Conclusions

References

Tables

Figures

◀

▶

◀

▶

Back

Close

Full Screen / Esc

Printer-friendly Version

Interactive Discussion



fitted O_2O_2 ΔSCD is buffered by the fact that the integral O_2O_2 absorption (integral over the wavelength window of each band) does not depend on temperature (Thalman and Volkamer, 2013). The temperature induced corrections required to bring DS and AMAX-DOAS VCDs to the model values are significantly smaller than the corrections reported for the boundary layer MAX-DOAS observations in the literature (0.94 ± 0.02 vs. 0.75 ± 0.1 , see Table 1).

When using two σ (203 and 293 K) the temperature dependent bias in the measured VCDs is essentially zero within errors at 477 nm. This illustrates the importance of (1) accounting for the temperature dependence of the O_2O_2 cross section during the DOAS fit and (2) accurately representing the atmosphere in the RTM (results including aerosol are better compared to the Rayleigh case).

The UV region, however, is more sensitive to the DOAS fitting parameters and does not show a clear improvement in the retrieved VCDs while using two σ (203 and 293 K). This is especially pronounced for DS measurements (Fig. 8) where several percent underestimation of the VCD is observed. AMAX-DOAS data seem to be less sensitive and show only a few percent underestimations that are insignificant within the low error bars.

4.5 Error analysis of DS and AMAX-DOAS data

4.5.1 Direct Sun DOAS errors

The main source of error in DS $\tau(\text{O}_2\text{O}_2)$ measurements is DOAS fitting error of $\Delta\text{SCD}(\text{O}_2\text{O}_2)$. Since DS $\text{AMF}(\text{O}_2\text{O}_2)$ is wavelength independent at most SZA, retrieval in any of the wavelength regions where O_2O_2 has a significant absorption should produce the same ΔSCD . In practice, DOAS fitting parameters such as order of the polynomial function, mimicking Rayleigh and Mie extinction, exact fitting window boundaries, offset correction, uncertainties in cross sections of other trace gases absorbing in the same wavelength region, errors in instrument transfer function and wavelength

calibration introduce errors in ΔSCD . Table 5 summarizes DS normalized $\tau(\text{O}_2\text{O}_2)$ errors calculated for different DOAS fitting scenarios accounting for variability in CD.

An error associated with DS AMF comes from the uncertainty in SZA ephemeris and O_2O_2 effective height calculation. The error in SZA calculation is 0.02° and error in O_2O_2 effective height is less than 200 m. This translates to an error of less than 0.1 % at $\text{SZA} < 80^\circ$ which increases to 2 % at 88° SZA. Since most measurements contributing to the final results come from the observations at $\text{SZA} < 80^\circ$ we assume AMF error of 0.1 %.

Error in the total CD^* calculated from the T , P , SH profiles is determined as one standard deviation of CD^* variability at a specific T . Yearly average relative error is about 1.6 %

To evaluate ΔSCD and SCD_{REF} errors associated with the DOAS fitting parameters we varied the wavelength fitting windows (visible: 435–485, 445–485, 460–490; UV: 350–385, 350–370, 335–370, 335–390 nm), polynomial order (3, 4 and 5, depending on the $\Delta\lambda$), offset order (0 and 1), and $\sigma(\text{O}_3)$ (single temperature vs. two temperatures). One standard deviation of the SCD_{REF} derived from all fitting scenarios is reported as SCD_{REF} error. For the visible spectral window this is about 1 % and 2.4 % for the UV.

The noise in the residual OD (Eq. 3) was significantly reduced by averaging daily measurements. This resulted in SNR increase in irradiance between 5–27 times depending on the observation schedule.

The total error in the normalized daily VOD and VCD is derived from the DOAS sensitivity scenarios and $\text{CD}^* \pm 1.6\%$ as one standard deviation. It is about 3.5 % for UV and 2.1 % for the visible wavelength regions.

4.5.2 Aircraft MAX-DOAS

The DOAS fitting error of $\Delta\text{SCD}(\text{O}_2\text{O}_2)$ is the main error source for the AMAX-DOAS data. Error values listed in Table 5 are representative for individual measurements with a 15 s time resolution. Statistical averaging of individual spectra can be used to further reduce this error. The total errors of 5.2 % at 360 nm and 2.4 % at 477 nm are therefore

Absorption with significant pressure and temperature differences

E. Spinei et al.

Title Page

Abstract

Introduction

Conclusions

References

Tables

Figures

◀

▶

◀

▶

Back

Close

Full Screen / Esc

Printer-friendly Version

Interactive Discussion



Absorption with significant pressure and temperature differences

E. Spinei et al.

upper limits, particularly in the UV. AMAX-DOAS data shown in Figs. 6 and 8 is taken from EA 0° measurements only. Unlike for the DS measurements, Eq. (3) was directly applied to the AMAX-DOAS Δ SCD results without prior averaging. To reduce scatter VOD and VCD data included in Figs. 6 and 8 are averages and standard deviations of binned data in 2 K increments. The AMF error is due to the statistical nature of the Monte Carlo RTM McArtim (statistical uncertainty). McArtim was initiated several times with identical settings and variations are small. The error in the total O₂O₂ CD* is directly representative of the error in our temperature measurements; errors due to pressure measurements are negligible. The major source of uncertainty is related to assumptions about SCD_{REF}. We assess this error by determining SCD_{REF} experimentally from the offsets of linear fits of measured Δ SCD(O₂O₂) over modeled SCD(O₂O₂) as shown in Fig. 3 and detailed in Table 4. These offsets agree within error bars with those computed from RTM for a Rayleigh atmosphere, or for an atmosphere containing aerosols (see Table 4).

The excellent agreement between DS DOAS (no RTM) and AMAX-DOAS (uses RTM) is not trivial, given the need for radiative transfer calculations, and active control of telescope pointing with AMAX-DOAS observations (Baidar et al., 2013). For example, a 1 % uncertainty in the Rayleigh scattering cross section used in the RTM directly translates into an error of the same order in the predicted O_2O_2 SCD. A recent laboratory study extends knowledge about Rayleigh scattering cross sections at UV wavelengths (Thalman et al., 2014), and confirms that the cross sections that underlie our RTM are correct within very small error bounds ($< 1\%$). This is noteworthy, since variations in the Rayleigh scattering cross-sections had been found around 4 % at 477 nm when comparing empirical fits of previous measurements in the literature with theory (Thalman et al., 2014). We conclude that any systematic bias from using the RTM to interpret the AMAX-DOAS measurements is not due to the representation of Rayleigh scattering, and limited by the small remaining uncertainty due to aerosols. Missing knowledge on aerosol distribution and properties in the atmosphere presents a fundamental limitation to determining SCD_{REF} for AMAX-DOAS measurements.

The difference in SCD_{REF} between a Rayleigh or aerosol atmosphere introduces a systematic error of about 2 % in modeled VCD and VOD values (see Figs. 6 and 8). We consider this to be the limit at which our data can be considered accurate. The overall errors for both DS and AMAX-DOAS are comparable, particularly after averaging of

AMAX-DOAS $\Delta SCD(O_2O_2)$.

5 Summary

This study presents DS and AMAX-DOAS measurements of O_2O_2 absorption optical depths under actual Earth atmospheric conditions in two wavelength regions (335–390 nm and 435–490 nm). DS irradiance measurements were made by the research grade MFDOAS instrument from 2007 to 2014 at seven sites with significant pressure (778–1020 hPa) and O_2O_2 profile weighted temperature (247–275 K) differences. Aircraft MAX-DOAS measurements were conducted by the University of Colorado airborne MAX-DOAS instrument on 29 January 2012 over the Southern Hemisphere subtropical Pacific Ocean. Scattered solar radiance spectra were collected at altitudes between 9 and 13.2 km, with O_2O_2 effective temperatures of 231–244 K, and near pure Rayleigh scattering conditions. The data were evaluated to understand temperature and pressure dependence of the O_2O_2 molecular absorption cross section using vertical O_2O_2 column densities calculated from atmospheric sounding, in-situ data and/or model temperature and pressure profiles adjusted by the surface observations.

DS data interpretation involves a simple geometric calculation of AMF. AMAX-DOAS observations, on the other hand, require RT modeling of atmospheric conditions to estimate AMF.

Based on the atmospheric DS observations, there is no pressure dependence of the O_2O_2 cross section within MFDOAS errors (3 %). A temperature dependence in $\sigma(O_2O_2)$ from 231 to 275 K was observed at about 9 ± 2.5 % per 44 K rate in both wavelength regions from DS and AMAX-DOAS measurements. The change in band shape described by Thalman and Volkamer (2013) was observed under atmospheric

Absorption with significant pressure and temperature differences

E. Spinei et al.

Title Page

Abstract

Introduction

Conclusions

References

Tables

Figures

◀

▶

◀

▶

Back

Close

Full Screen / Esc

Printer-friendly Version

Interactive Discussion



conditions in both DS and AMAX-DOAS datasets. Derived peak O_2O_2 cross sections of 360 and 477 nm bands were compared to the recent laboratory measured O_2O_2 cross sections of Thalman and Volkamer (2013) at 233, 253 and 273 K. The agreement between the peak O_2O_2 cross sections at both wavelengths is within 3 %.

The combined observations of DS and AMAX-DOAS measurements support the fact that laboratory measured O_2O_2 cross sections are well suited for DOAS observations under typical atmospheric conditions.

The effect of $\sigma(\text{O}_2\text{O}_2)$ temperature dependence on the fitted $\text{O}_2\text{O}_2 \Delta\text{SCD}$ is buffered by the fact that the integral O_2O_2 absorption (integral over the wavelength window of each band) does not depend on temperature (Thalman and Volkamer, 2013). SCD retrieved from DS and AMAX-DOAS measurements were within 6 % of the model/ T , P , SH SCD even at temperatures below 250 K. This suggests that $\sigma(\text{O}_2\text{O}_2)$ cross sections do not contribute to creating the need for correction factors of 25 ± 10 % reported in the literature for some PBL MAX-DOAS measurements where the effective O_2O_2 temperatures are expected to be between 265 K (zenith) to 275 K ($1\text{--}2^\circ$ EA).

T -dependent bias in ΔSCD can be reduced by simultaneously fitting $\sigma(\text{O}_2\text{O}_2)$ at different temperatures, which becomes increasingly important for measurements with effective O_2O_2 temperatures below 250 K as is the case for AMAX-DOAS measurements. Fitting $\sigma(\text{O}_2\text{O}_2)$ at 203 and 293 K improved AMAX-DOAS results in both UV and visible wavelength regions.

Acknowledgements. The MFDOAS development and deployment were supported by the National Aeronautics and Space Administration grants to Washington State University (NNX09AJ28G and NNG05GR56G). We thank the institutional support from JPL Table Mountain Facility (Stanley Sander et al.), UAF (William Simpson et al.), GSFC, Cabauw (CINDI organizers), UAH (M. Newchurch et al.), PNNL (Jim Mather et al.) where the field measurements were made. Ozone sonde measurements were supported through NOAA.

The TORERO project is funded by the National Science Foundation under award AGS-1104104 (PI: R. Volkamer). The involvement of the NSF-sponsored Lower Atmospheric Observing Facilities, managed and operated by the National Center for Atmospheric Research (NCAR) Earth Observing Laboratory (EOL), is acknowledged. R. Volkamer acknowledges

Absorption with significant pressure and temperature differences

E. Spinei et al.

Title Page

Abstract

Introduction

Conclusions

References

Tables

Figures

◀

▶

◀

▶

Back

Close

Full Screen / Esc

Printer-friendly Version

Interactive Discussion



financial support from a NSF Faculty Early Career Development (CAREER) award ATM-0847793 to develop the CU AMAX-DOAS instrument. S. Baidar is a recipient of ESRL/CIRES graduate fellowship. I. Ortega is a recipient of a NASA graduate fellowship. The authors thank Brad Pierce for RAQMS model data used to constrain McArtim, and Tim Deutschman for providing McArtim.

References

- Acarreta, J. R., De Haan, J. F., and Stammes, P.: Cloud pressure retrieval using the O₂-O₂ absorption band at 477 nm, *J. Geophys. Res.*, 109, D05204, doi:10.1029/2003JD003915, 2004.
- Baidar, S., Oetjen, H., Coburn, S., Dix, B., Ortega, I., Sinreich, R., and Volkamer, R.: The CU Airborne MAX-DOAS instrument: vertical profiling of aerosol extinction and trace gases, *Atmos. Meas. Tech.*, 6, 719–739, doi:10.5194/amt-6-719-2013, 2013.
- Bogumil, K.: Measurements of molecular absorption spectra with the SCIAMACHY pre-flight model: instrument characterization and reference data for atmospheric remote-sensing in the 230–2380 nm region, *J. Photoch. Photobio. A*, 157, 167–184, doi:10.1016/S1010-6030(03)00062-5, 2003.
- Cede, A., Herman, J., Richter, A., Krotkov, N., and Burrows, J.: Measurements of nitrogen dioxide total column amounts using a Brewer double spectrophotometer in direct Sun mode, *J. Geophys. Res.*, 111, D05304, doi:10.1029/2005JD006585, 2006.
- Clémer, K., Van Roozendael, M., Fayt, C., Hendrick, F., Hermans, C., Pinardi, G., Spurr, R., Wang, P., and De Mazière, M.: Multiple wavelength retrieval of tropospheric aerosol optical properties from MAXDOAS measurements in Beijing, *Atmos. Meas. Tech.*, 3, 863–878, doi:10.5194/amt-3-863-2010, 2010.
- Curier, R. L., Veefkind, J. P., Braak, R., Veihelmann, B., Torres, O., and de Leeuw, G.: Retrieval of aerosol optical properties from OMI radiances using a multiwavelength algorithm: application to western Europe, *J. Geophys. Res.*, 113, D17S90, doi:10.1029/2007JD008738, 2008.
- Danckaert, T., Fayt, C., Van Roozendael, M., De Smedt, I., Letocart, V., Merlaud, A., and Pinardi, G.: QDOAS Software User Manual, Belgian Institute for Space Aeronomy (BIRA-IASB), 2012.

Absorption with significant pressure and temperature differences

E. Spinei et al.

Title Page

Abstract

Introduction

Conclusions

References

Tables

Figures

◀

▶

◀

▶

Back

Close

Full Screen / Esc

Printer-friendly Version

Interactive Discussion



- Daumont, D., Brion, J., Charbonnier, J., and Malicet, J.: Ozone UV spectroscopy I: absorption cross-sections at room temperature, *J. Atmos. Chem.*, 15, 145–155, doi:10.1007/BF00053756, 1992.
- Denning, R. F., Guidero, S. L., Parks, G. S., and Gary, B. L.: Instrument description of the airborne microwave temperature profiler, *J. Geophys. Res.*, 94, 16757, doi:10.1029/JD094iD14p16757, 1989.
- Deutschmann, T., Beirle, S., Frieß, U., Grzegorski, M., Kern, C., Kritten, L., Platt, U., Prados-Román, C., Pukl[†]te, J., Wagner, T., Werner, B., and Pfeilsticker, K.: The Monte Carlo atmospheric radiative transfer model McArtim: introduction and validation of Jacobians and 3-D features, *J. Quant. Spectrosc. Ra.*, 112, 1119–1137, doi:10.1016/j.jqsrt.2010.12.009, 2011.
- Dix, B., Baidar, S., Bresch, J. F., Hall, S. R., Schmidt, K. S., Wang, S., and Volkamer, R.: Detection of iodine monoxide in the tropical free troposphere, *P. Natl. Acad. Sci. USA*, 110, 2035–2040, doi:10.1073/pnas.1212386110, 2013.
- Eloranta, E. W., Razenkov, I. A., Hedrick, J., and Garcia, J. P.: The Design and Construction of an Airborne High Spectral Resolution Lidar, in: *IEEE*, 1–6, 2008.
- Fayt, C. and Van Roozendael, M.: winDOAS 2.1 Software User Manual, BIRA-IASB, Uccle, Belgium, 2001.
- Fleischmann, O. C., Hartmann, M., Burrows, J. P., and Orphal, J.: New ultraviolet absorption cross-sections of BrO at atmospheric temperatures measured by time-windowing Fourier transform spectroscopy, *J. Photoch. Photobio. A*, 168, 117–132, doi:10.1016/j.jphotochem.2004.03.026, 2004.
- Frieß, U., Monks, P. S., Remedios, J. J., Rozanov, A., Sinreich, R., Wagner, T., and Platt, U.: MAX-DOAS O₄ measurements: a new technique to derive information on atmospheric aerosols: 2. Modeling studies, *J. Geophys. Res.*, 111, D17S90, doi:10.1029/2005JD006618, 2006.
- Greenblatt, G. D., Orlando, J. J., Burkholder, J. B., and Ravishankara, A. R.: Absorption measurements of oxygen between 330 and 1140 nm, *J. Geophys. Res.*, 95, 18577–18582, doi:10.1029/JD095iD11p18577, 1990.
- Hermans, C.: O₄ absorption cross-sections at 296 K (335.59–666.63 nm), available at: <http://spectrolab.aeronomie.be/index.htm> (last access: 15 January 2011), 2011.
- Hermans, C., Vandaele, A., Carleer, M., Fally, S., Colin, R., Jenouvrier, A., Coquart, B., and Mérienne, M.-F.: Absorption cross-sections of atmospheric constituents: NO₂, O₂, and H₂O, *Environ. Sci. Pollut. R.*, 6, 151–158, doi:10.1007/BF02987620, 1999.

Absorption with significant pressure and temperature differences

E. Spinei et al.

Title Page

Abstract

Introduction

Conclusions

References

Tables

Figures

◀

▶

◀

▶

Back

Close

Full Screen / Esc

Printer-friendly Version

Interactive Discussion



Absorption with significant pressure and temperature differences

E. Spinei et al.

Title Page

Abstract

Introduction

Conclusions

References

Tables

Figures

◀

▶

◀

▶

Back

Close

Full Screen / Esc

Printer-friendly Version

Interactive Discussion



- Irie, H., Kanaya, Y., Akimoto, H., Iwabuchi, H., Shimizu, A., and Aoki, K.: First retrieval of tropospheric aerosol profiles using MAX-DOAS and comparison with lidar and sky radiometer measurements, *Atmos. Chem. Phys.*, 8, 341–350, doi:10.5194/acp-8-341-2008, 2008.
- Irie, H., Kanaya, Y., Akimoto, H., Iwabuchi, H., Shimizu, A., and Aoki, K.: Dual-wavelength aerosol vertical profile measurements by MAX-DOAS at Tsukuba, Japan, *Atmos. Chem. Phys.*, 9, 2741–2749, doi:10.5194/acp-9-2741-2009, 2009.
- Lim, B., Mahoney, M., Haggerty, J., and Denning, R.: The Microwave Temperature Profiler performance in recent airborne campaigns, *Geosci. Remote. Sens. Symposium (IGARSS)*, 3363–3366, 2013.
- Malicet, J., Daumont, D., Charbonnier, J., Parisse, C., Chakir, A., and Brion, J.: Ozone UV spectroscopy. II. Absorption cross-sections and temperature dependence, *J. Atmos. Chem.*, 21, 263–273, doi:10.1007/BF00696758, 1995.
- Massie, S. T. and Hervig, M.: HITRAN 2012 refractive indices, *J. Quant. Spectrosc. Ra.*, 130, 373–380, doi:10.1016/j.jqsrt.2013.06.022, 2013.
- Meller, R. and Moortgat, G. K.: Temperature dependence of the absorption cross sections of formaldehyde between 223 and 323 K in the wavelength range 225–375 nm, *J. Geophys. Res.*, 105, 7089–7101, doi:10.1029/1999JD901074, 2000.
- Merlaud, A., Van Roozendaal, M., Theys, N., Fayt, C., Hermans, C., Quennehen, B., Schwarzenboeck, A., Ancellet, G., Pommier, M., Pelon, J., Burkhardt, J., Stohl, A., and De Mazière, M.: Airborne DOAS measurements in Arctic: vertical distributions of aerosol extinction coefficient and NO₂ concentration, *Atmos. Chem. Phys.*, 11, 9219–9236, doi:10.5194/acp-11-9219-2011, 2011.
- Newnham, D. A. and Ballard, J.: Visible absorption cross sections and integrated absorption intensities of molecular oxygen (O₂ and O₄), *J. Geophys. Res.*, 103, 28801–28815, doi:10.1029/98JD02799, 1998.
- Osterkamp, H., Ferlemann, F., Harder, H., Perner, D., Platt, U., and Schneider, M.: First measurement of the atmospheric O₄ profile, in: *Proceedings of the 4th European Symposium on Polar stratospheric ozone 1997*, Schliersee/Germany, 478–481, Luxembourg: European Commission, 1997.
- Pfeilsticker, K., Bösch, H., Camy-Peyret, C., Fitzenberger, R., Harder, H., and Osterkamp, H.: First atmospheric profile measurements of UV/visible O₄ absorption band intensities: implications for the spectroscopy, and the formation enthalpy of the O₂O₂ dimer, *Geophys. Res. Lett.*, 28, 4595, doi:10.1029/2001GL013734, 2001.

Absorption with significant pressure and temperature differences

E. Spinei et al.

Title Page

Abstract

Introduction

Conclusions

References

Tables

Figures

◀

▶

◀

▶

Back

Close

Full Screen / Esc

Printer-friendly Version

Interactive Discussion



- Platt, U.: Differential Optical Absorption Spectroscopy (DOAS), in: Air Monitoring by Spectroscopic Techniques, Vol. 127, edited by: Sigrist, M. W., Wiley-IEEE, New York, 531, 1994.
- Rothman, L. S., Gordon, I. E., Barber, R. J., Dothe, H., Gamache, R. R., Goldman, A., Perevalov, V. I., Tashkun, S. A., and Tennyson, J.: HITEMP, the high-temperature molecular spectroscopic database, J. Quant. Spectrosc. Ra., 111, 2139–2150, doi:10.1016/j.jqsrt.2010.05.001, 2010.
- Salow, H. and Steiner, W.: Absorption spectrum of oxygen at high pressures and the existence of O₄ molecules, Nature, 134, 463–463, doi:10.1038/134463a0, 1934.
- Sneep, M. and Ubachs, W.: Cavity ring-down measurement of the O₂–O₂ collision-induced absorption resonance at 477 nm at sub-atmospheric pressures, J. Quant. Spectrosc. Ra., 78, 171–178, doi:10.1016/S0022-4073(02)00190-5, 2003.
- Sneep, M., Ityakov, D., Aben, I., Linnartz, H., and Ubachs, W.: Temperature-dependent cross sections of O₂–O₂ collision-induced absorption resonances at 477 and 577 nm, J. Quant. Spectrosc. Ra., 98, 405–424, doi:10.1016/j.jqsrt.2005.06.004, 2006.
- Sneep, M., de Haan, J. F., Stammes, P., Wang, P., Vanbaucse, C., Joiner, J., Vasilkov, A. P., and Levelt, P. F.: Three-way comparison between OMI and PARASOL cloud pressure products, J. Geophys. Res., 113, D15S23, doi:10.1029/2007JD008694, 2008.
- Thalman, R. and Volkamer, R.: Temperature dependent absorption cross-sections of O₂–O₂ collision pairs between 340 and 630 nm and at atmospherically relevant pressure, Phys. Chem. Chem. Phys., 15, 15371, doi:10.1039/c3cp50968k, 2013.
- Thalman, R., Zarzana, K., Tolbert, M. A., and Volkamer, R.: Rayleigh scattering cross-section measurements of nitrogen, argon, oxygen and air, J. Quant. Spectr. Radiat. Trans., 147, 171–178, doi:10.1016/j.jqsrt.2014.05.030, 2014.
- Vandaele, A., Hermans, C., Simon, P., Carleer, M., Colin, R., Fally, S., Mérienne, M.-F., Jenouvrier, A., and Coquart, B.: Measurements of the NO₂ absorption cross-section from 42 000 cm^{–1} to 10 000 cm^{–1} (238–1000 nm) at 220 K and 294 K, J. Quant. Spectrosc. Ra., 59, 171–184, doi:10.1016/S0022-4073(97)00168-4, 1998.
- Vandaele, A. C., Hermans, C., Fally, S., Carleer, M., Mérienne, M.-F., Jenouvrier, A., Coquart, B., and Colin, R.: Absorption cross-sections of NO₂: simulation of temperature and pressure effects, J. Quant. Spectrosc. Ra., 76, 373–391, doi:10.1016/S0022-4073(02)00064-X, 2003.

Volkamer, R.: Absorption von Sauerstoff im Herzberg I System und Anwendungen auf die Aromatenmessungen am EUROpran PHOto REactor (EUPHORE), Diploma thesis, Univ. of Heidelberg, Germany, 1996.

Wagner, T., Friedeburg, C. von, Wenig, M., Otten, C., and Platt, U.: UV-visible observations of atmospheric O₄ absorptions using direct moonlight and zenith-scattered sunlight for clear-sky and cloudy sky conditions, J. Geophys. Res., 107, 4424, doi:10.1029/2001JD001026, 2002.

Wagner, T., Dix, B., Friedeburg, C. v., Frieß, U., Sanghavi, S., Sinreich, R., and Platt, U.: MAX-DOAS O₄ measurements: a new technique to derive information on atmospheric aerosols-Principles and information content, J. Geophys. Res.-Atmos., 109, 22205, doi:10.1029/2004JD004904, 2004.

Wilmouth, D. M., Hanisco, T. F., Donahue, N. M., and Anderson, J. G.: Fourier Transform Ultraviolet Spectroscopy of the A 2Π_{3/2} ← X 2Π_{3/2} Transition of BrO†, J. Phys. Chem.-USA, 103, 8935–8945, doi:10.1021/jp991651o, 1999.

AMTD

7, 10015–10057, 2014

Absorption with significant pressure and temperature differences

E. Spinei et al.

Title Page

Abstract

Introduction

Conclusions

References

Tables

Figures

◀

▶

◀

▶

Back

Close

Full Screen / Esc

Printer-friendly Version

Interactive Discussion



Absorption with significant pressure and temperature differences

E. Spinei et al.

Title Page

Abstract

Introduction

Conclusions

References

Tables

Figures

◀

▶

◀

▶

Back

Close

Full Screen / Esc

Printer-friendly Version

Interactive Discussion



Table 2. O₂O₂ vertical column density and effective temperature at the observation sites during Direct Sun and aircraft MAX-DOAS measurement periods.

	Site name and location	Alt., site P [km hPa ⁻¹]	Observation period	Mean O ₂ O ₂ CD* × 10 ⁴³ [molecules ² cm ⁻⁵]	AMF _{REF}	T_{REF}^* [K]	Mean O ₂ O ₂ $T^* \pm \sigma$ [K]
Direct Sun	JPL, CA 34.38° N 117.68° W	2.285, 779 ± 1	2–11 Jul 2007	0.767 ± 0.004	1.02	265 ± 1	264.39 ± 0.42
	WSU, Pullman, WA 46.733° N 117.169° W	0.764, 913 ± 3	Sep–Nov 2007 Jul–Nov 2011	1.115 ± 0.030 1.097 ± 0.030	1.35 1.16	269 ± 1 268 ± 1	259.61 ± 4.85 262.84 ± 5.70
	UAF, Fairbanks, AK 64.859° N 147.85° E	0.224, 985 ± 10	27 Mar– 9 Apr 2011	1.288 ± 0.033	1.96	253 ± 1	250.35 ± 2.10
	UAH, Huntsville, AL 34.725° N 86.645° W	0.223, 977 ± 3	9–18 Aug 2008	1.208 ± 0.012	1.09	271 ± 1	271.16 ± 1.02
	PNNL, Richland, WA 46.3409° N 119.279° W	0.126, 1000 ± 25	15 Apr– 30 Jun 2008	1.28 ± 0.03	1.06 1.09	265 ± 1	264.09 ± 5.14
	NASA/GSFC Greenbelt, MD 38.993° N 76.839° W	0.090, 1011 ± 7	May 2007 Oct 2012– Mar 2014	1.278 ± 0.02 1.299 ± 0.04	1.06 1.09	267 ± 1 266 ± 1	262.93 ± 6.51
	Cabauw, the Netherlands 51.971° N 4.927° E	~ 0 1020 ± 5	16 Jun– 5 Jul 2009	1.28 ± 0.02	1.14	269 ± 1	266.97 ± 2.85
Aircraft MAX-DOAS	Subtropical Pacific Ocean 29.7–29.9° S 92.4–92.1° E	9–13.2, 321–174	18:06– 18:30 UTC 29 Jan 2012	1.29	VIS: 0.98 UV: 0.89	VIS: 252.4 ± 0.2 UV: 247.6 ± 0.2	VIS: 236.3 ± 5.2 UV: 238.6 ± 3.2

Absorption with significant pressure and temperature differences

E. Spinei et al.

Title Page

Abstract

Introduction

Conclusions

References

Tables

Figures

◀

▶

◀

▶

Back

Close

Full Screen / Esc

Printer-friendly Version

Interactive Discussion



Table 3. DOAS analysis parameters used in direct sun and aircraft MAX-DOAS analysis.

	Direct sun		Aircraft MAX-DOAS	
Fitting window	335–388 nm ¹ 350–385 nm ²	435–490 nm	350–387.5 nm Gap: 366–374.5 nm	445–485 nm
BrO	223 K, Fleischmann et al. (2004)	–	228 K, Wilmouth et al. (1999)	–
HCHO	298 K, Meller and Moortgat (2000)	–	298 K, Meller and Moortgat (2000)	–
H ₂ O	–	296 K, HITEMP (2010)	–	296 K, HITEMP (2010); H ₂ O lab ³
O ₃	228 and 243 K, Daumont, Brion, Malicet		223 K, Bogumil et al. (2003)	
NO ₂	linear model, Vandaele et al. (2003)		220 K, Vandaele et al. (1998)	
O ₂ O ₂	296 K, Hermans et al. (2011)		296 K, Hermans et al. (2011) 203 K and 293, Thalman and Volkamer (2013)	
Ring	–		Ring at 250 K from reference Ring at 220 K from 2nd reference	
Polynomial order	4 ¹ , 3 ²	5		5
Offset		slope		slope

¹ Spectra with U340 filter.

² Spectra without any filters.

³ Cross section recorded with AMAX-DOAS instrument at room temperature through an LED cavity system in the laboratory (Thalman and Volkamer, 2013).

Absorption with significant pressure and temperature differences

E. Spinei et al.

Title Page

Abstract

Introduction

Conclusions

References

Tables

Figures

◀

▶

◀

▶

Back

Close

Full Screen / Esc

Printer-friendly Version

Interactive Discussion



Table 4. Linear correlation parameters between AMAX-DOAS O_2O_2 ΔSCD using Hermans et al. (2011), 296 K σ /Thalman and Volkamer (2013) 203 K and 293 σ , and McArtim modeled SCDs.

	Pure Rayleigh Scattering		Rayleigh with aerosols Scattering	
	350–387.5, 360	445–485, 477	350–387.5, 360	445–485, 477
Fitting window, model wavelength [nm]				
R^2	1.00/0.98	1.00/1.00	0.99/0.98	1.00/0.99
Slope*	1.029 ± 0.049/ 0.957 ± 0.044	1.016 ± 0.01/ 0.986 ± 0.008	1.052 ± 0.050/ 0.978 ± 0.045	1.026 ± 0.01/ 0.996 ± 0.01
Intercept * × 10 ⁴³ [molecules ² cm ⁻⁵]	1.13 ± 0.11/ 1.07 ± 0.09	1.23 ± 0.03/ 1.25 ± 0.03	1.18 ± 0.08/ 1.12 ± 0.08	1.27 ± 0.03/ 1.29 ± 0.03
Modeled SCD _{REF} × 10 ⁴³ [molecules ² cm ⁻⁵]	1.15	1.25	1.17	1.28

* ± standard deviation.

Table 5. Error budget of the 360 and 477 nm band peak O₂O₂ $\sigma(T)$ derived from DS and AMAX-DOAS measurements.

	Error source	Error Peak of 360 nm band	Error Peak of 477 nm band
Direct sun DOAS	O ₂ O ₂ profile weighted temperature	1 K	1 K
	O ₂ O ₂ AMF	0.1 %	0.1 %
	O ₂ O ₂ CD*	1.6 %	1.6 %
	O ₂ O ₂ ΔSCD	< 2 %	< 1 %
	SCD _{ref}	2.4 %	0.8 %
	Total Error	3.5 %	2.1 %
Aircraft MAX-DOAS	O ₂ O ₂ profile weighted temperature	1 K	1 K
	O ₂ O ₂ ΔAMF	0.4 %	0.4 %
	O ₂ O ₂ CD*	0.8 %	0.8 %
	O ₂ O ₂ ΔSCD	3.8 %	2.0 %
	SCD _{ref}	< 6.8 % ^a < 3.5 % ^b	< 2.3 % ^a < 0.9 % ^b
	Total Error	< 5.2 %	< 2.4 %

^a Maximum relative error from Table 4.

^b Maximum relative error weighed by the relative contribution of the SCD_{ref} to the overall; SCD = dSCD + SCD_{ref}; weighed relative error = (SCD_{ref}/SCD) · SCD_{ref, error}; the ratio SCD_{ref}/SCD is on average 0.51 and 0.39 at 360 nm and 477 nm, respectively.

Absorption with significant pressure and temperature differences

E. Spinei et al.

Title Page

Abstract

Introduction

Conclusions

References

Tables

Figures



Back

Close

Full Screen / Esc

Printer-friendly Version

Interactive Discussion



Absorption with significant pressure and temperature differences

E. Spinei et al.

Title Page

Abstract

Introduction

Conclusions

References

Tables

Figures



[Back](#)

Close

Full Screen / Esc

[Printer-friendly Version](#)

Interactive Discussion

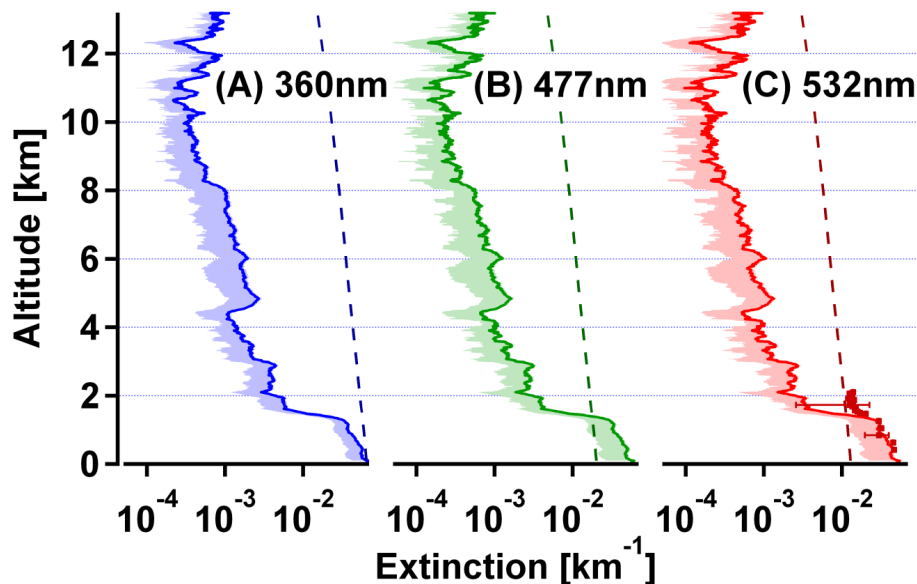


Figure 1. Vertical profiles of aerosol extinction at **(A)** 360 nm, **(B)** 477 nm, and **(C)** 532 nm during the AMAX-DOAS case study (solid lines) and HSRL measured extinction at 532 nm (Red squares); Mie calculations constrained by measured size distributions assuming “n” of sea salt; (shading) sensitivity studies assuming “n” of pure water; (dashed lines) extinction from Rayleigh scattering for air densities calculated from measured temperature, pressure, and water vapor profiles.

Absorption with significant pressure and temperature differences

E. Spinei et al.

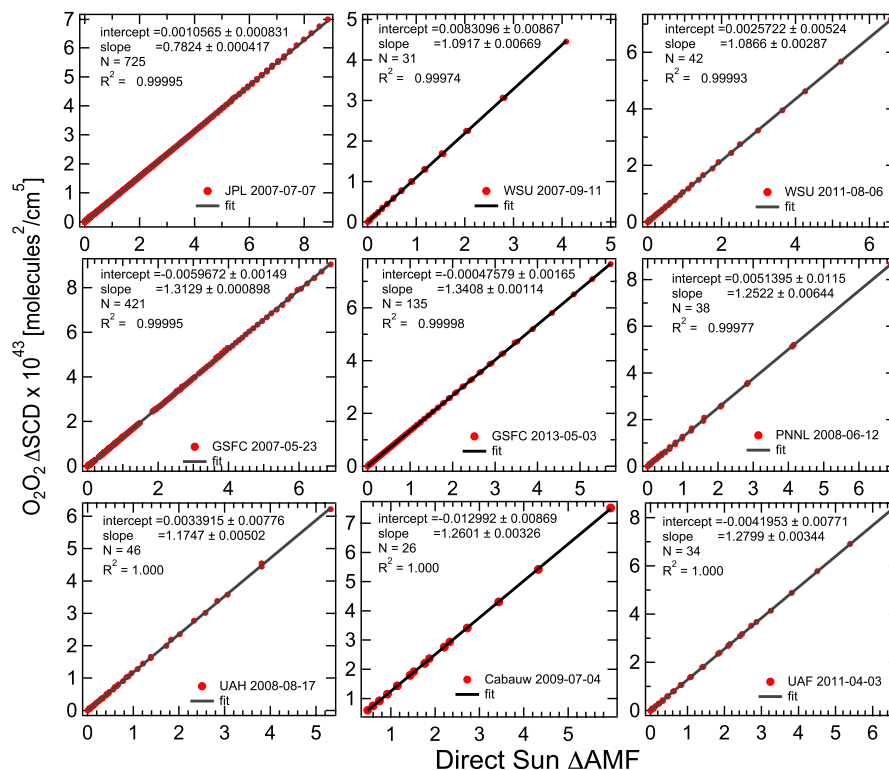


Figure 2. Linear regression between MFDOAS measured direct sun Δ SCD and Δ AMF (Langley Plot) to derive O_2O_2 SCD in the reference spectra at seven sites. Reference date is listed for each site. Correlation is calculated using the least square method. (Coefficient values $\pm 95\%$ confidence interval) $\times 10^{43}$ molecules² cm⁻⁵, number of measurements are shown. R^2 of the linear fit is > 0.9995 . Slope represents estimation of SCD_{REF} from 435–490 nm fitting window and DOAS fitting settings summarized in Table 3.

[Title Page](#)
[Abstract](#)
[Introduction](#)
[Conclusions](#)
[References](#)
[Tables](#)
[Figures](#)
[◀](#)
[▶](#)
[◀](#)
[▶](#)
[Back](#)
[Close](#)
[Full Screen / Esc](#)
[Printer-friendly Version](#)
[Interactive Discussion](#)


Absorption with significant pressure and temperature differences

E. Spinei et al.

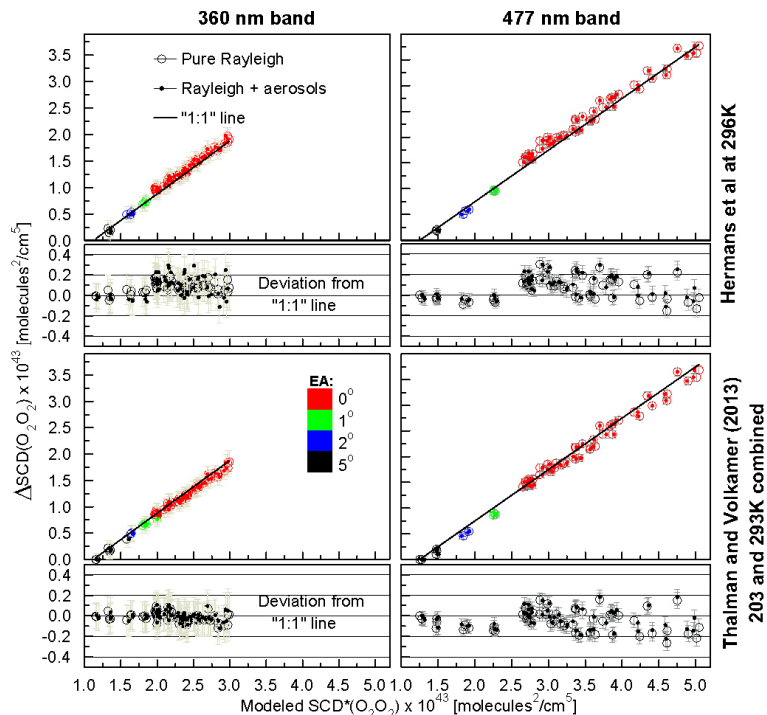


Figure 3. Measured Δ SCDs at 360 nm (left panel) and 477 nm (right panel) vs. modeled O_2O_2 SCD^* for a pure Rayleigh atmosphere and with aerosol profile using fitting parameters outlined in Table 3. Upper panel presents data using Hermans et al. (2011) $\sigma(\text{O}_2\text{O}_2)$ at 296 K, lower panel – combined Thalman and Volkamer (2013) at 203 and 293 K with their corresponding deviations from “1 : 1” line. Color code represents AMAX viewing elevation angles of individual data points. Error bars are based on 2 times fit residual rms to represent fit accuracy.

[Title Page](#)
[Abstract](#)
[Introduction](#)
[Conclusions](#)
[References](#)
[Tables](#)
[Figures](#)
[◀](#)
[▶](#)
[◀](#)
[▶](#)
[Back](#)
[Close](#)
[Full Screen / Esc](#)
[Printer-friendly Version](#)
[Interactive Discussion](#)


Absorption with significant pressure and temperature differences

E. Spinei et al.

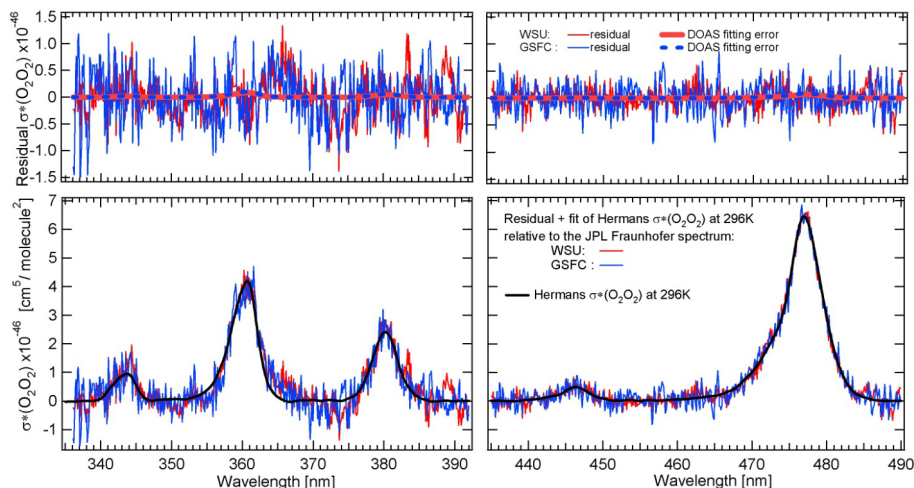


Figure 4. O_2O_2 “DOAS apparent” absorption cross section derived from the DS MFDOAS spectra (282–498 nm, no filters) collected over WSU, Pullman, WA (925 hPa, 11 September 2007) and GSFC, Greenbelt, MD (1013 hPa, 23 May 2007) relative to the reference spectrum collected over JPL (780 hPa, 7 July 2007) in UV and visible spectral windows.

[Title Page](#)[Abstract](#)[Introduction](#)[Conclusions](#)[References](#)[Tables](#)[Figures](#)[◀](#)[▶](#)[◀](#)[▶](#)[Back](#)[Close](#)[Full Screen / Esc](#)[Printer-friendly Version](#)[Interactive Discussion](#)

Absorption with significant pressure and temperature differences

E. Spinei et al.

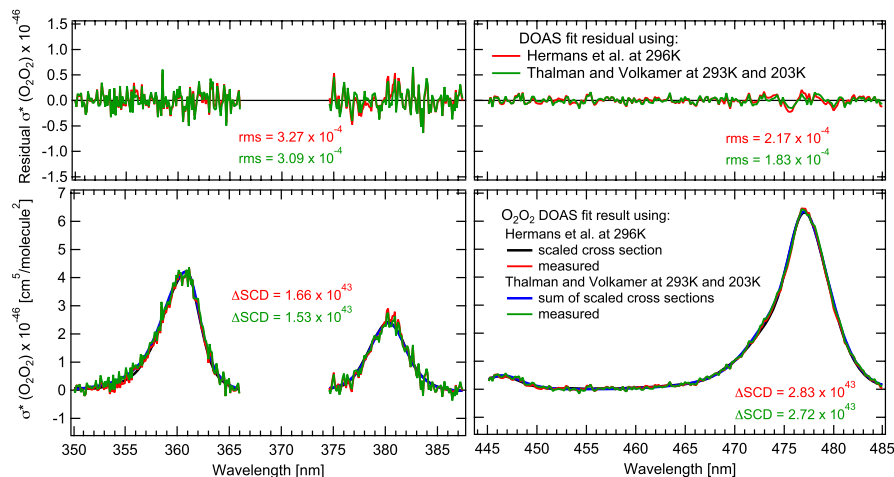


Figure 5. AMAX-DOAS spectral fit examples in UV and visible windows fitting (1) only one O_2O_2 cross section: Hermans et al. (2011) at 296 K, and (2) two O_2O_2 cross sections: Thalman and Volkamer (2013) at 203 and 293 K. The effective O_2O_2 temperatures for the displayed spectra are 239.7 ± 0.4 K at 360 and 234.8 ± 0.5 K at 477 nm.

Title Page

Abstract

Introduction

Conclusions

References

Tables

Figures

◀

▶

◀

▶

Back

Close

Full Screen / Esc

Printer-friendly Version

Interactive Discussion



Absorption with significant pressure and temperature differences

E. Spinei et al.

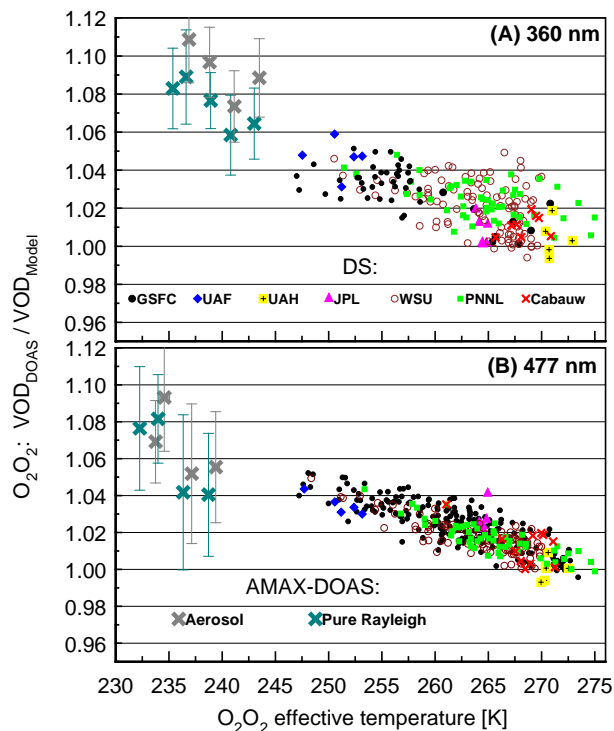


Figure 6. Vertical optical depth at 360 (A) and 477 nm (B), derived from DS and AMAX-DOAS measurements over all sites, and normalized by the VOD^* calculated from sonde/measured/model temperature, pressure and specific humidity profiles as a function of O_2O_2 effective temperature. AMAX-DOAS data is averaged and binned for 2 K increments for a pure Rayleigh atmosphere and including aerosols. Table 3 lists DOAS settings.

Title Page

Abstract

Introduction

Conclusions

References

Tables

Figures

◀

▶

◀

▶

Back

Close

Full Screen / Esc

Printer-friendly Version

Interactive Discussion



Absorption with significant pressure and temperature differences

E. Spinei et al.

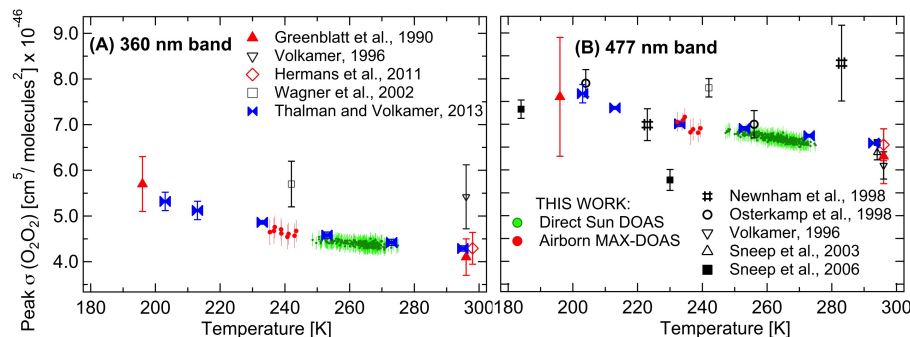


Figure 7. Collision induced absorption cross section of O_2O_2 at 360 (A) and 477 nm (B) recorded in literature since 1990 at their corresponding spectral resolutions. DS and AMAX DOAS derived peak cross sections (this work) are scaled to 0.3 nm FWHM, using Hermans et al. (2011) 296 K.

[Title Page](#)[Abstract](#)[Introduction](#)[Conclusions](#)[References](#)[Tables](#)[Figures](#)[◀](#)[▶](#)[◀](#)[▶](#)[Back](#)[Close](#)[Full Screen / Esc](#)[Printer-friendly Version](#)[Interactive Discussion](#)

Absorption with significant pressure and temperature differences

E. Spinei et al.

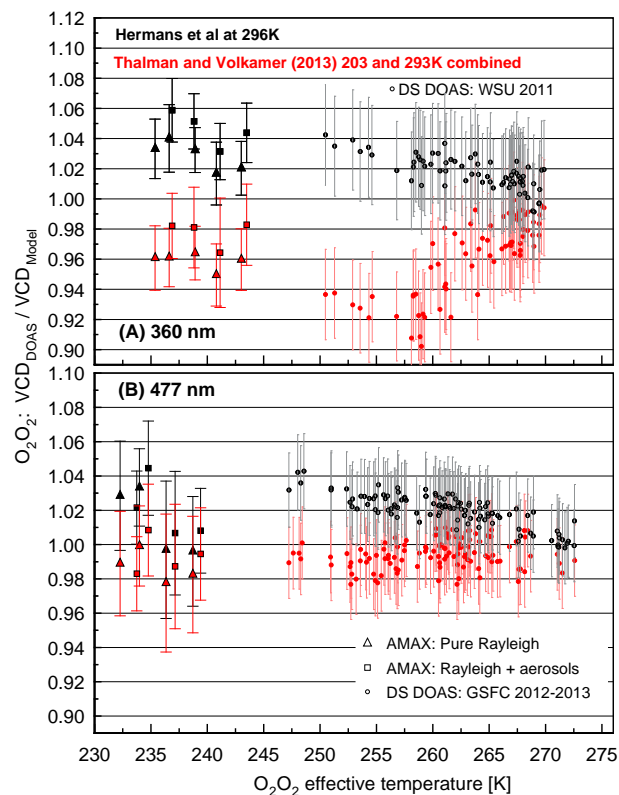


Figure 8. DS and AMAX-DOAS derived VCD from DOAS fitting in the UV **(A)** and visible **(B)** spectral windows using $\sigma(\text{O}_2\text{O}_2)$ by (1) Hermans et al. (2011) 296 (black symbols) and (2) Thalman and Volkamer (2013) at 203 and 293 K (red symbols), and normalized by VCD^* calculated from model (AMAX) and measured T , P and SH profiles. DS UV spectra, collected with U340 filter, were analyzed using AMAX-DOAS settings (Table 3). AMAX-DOAS data is averaged and binned for 2 K increments for a pure Rayleigh atmosphere and including aerosols.

[Title Page](#)
[Abstract](#)
[Introduction](#)
[Conclusions](#)
[References](#)
[Tables](#)
[Figures](#)
[◀](#)
[▶](#)
[◀](#)
[▶](#)
[Back](#)
[Close](#)
[Full Screen / Esc](#)
[Printer-friendly Version](#)
[Interactive Discussion](#)
